

03,05,07

Magnetotransport properties of α''' -(Cd_{0.5}Zn_{0.5})₃As₂ single crystals subjected to hydrostatic pressure

© L.A. Saypulaeva¹, V.S. Zakhvalinskii², A.G. Alibekov¹, Z.Sh. Pirmagomedov¹,
A.V. Kochura³, S.F. Marenkin⁴, A.I. Ril⁴

¹ Amirkhanov Institute of Physics, Dagestan Federal Research Center, Russian Academy of Sciences, Makhachkala, Russia

² Belgorod National Research University, Belgorod, Russia

³ Southwest State University, Kursk, Russia

⁴ Kurnakov Institute of General and Inorganic Chemistry, Russian Academy of Sciences, Moscow, Russia

E-mail: l.saypulaeva@gmail.com

Received November 25, 2023

Revised November 25, 2023

Accepted November 27, 2023

In α''' -(Cd_{0.5}Zn_{0.5})₃As₂, the effect of high hydrostatic pressure up to 9 GPa on the transport and field dependence of the transverse magnetoresistance has been investigated. This structure is tetragonal (p.g. $I4_1/amd$) with parameters $a = b = 8.55 \text{ \AA}$ and $c = 24.13 \text{ \AA}$. A Toroid-type chamber was used to generate high pressure. It is shown that increasing the pressure leads to suppression of positive magnetoresistance. In the phase transition region, the negative magnetoresistance at pressure $P \approx 5.4 \text{ GPa}$ in a 5 kOe field takes a minimum value approximately equal to -0.15 .

Keywords: high pressure, semiconductor, specific electrical resistance, Hall coefficient, magnetoresistance.

DOI: 10.61011/PSS.2024.01.57851.264

1. Introduction

The purpose of the study was to investigate the effect of environmental factors — temperature, pressure and magnetic field on the magnetotransport properties α''' -(Cd_{0.5}Zn_{0.5})₃As₂.

The earliest data on Cd₃As₂–Zn₃As₂ solid solutions are reported in [1–5]. It was found that these alloys are semiconductors: n -type ($0 \leq x \leq 1.35$) and p -type ($1.5 \leq x \leq 3$). Band parameters, effective electron and hole masses were calculated depending on the temperature and composition.

In [5–8], the effect of hydrostatic pressure up to 12000 bar on the electrophysical properties of Cd_{3–x}Zn_xAs₂ at room temperature was studied. It is shown that the experimental data may be explained according to the band structure model of Cd₃As₂ and Zn₃As₂ [9]. Special focus is made on Cd_{2.8}Zn_{0.2}As₂ alloy where researchers [1,10] observed the maximum Hall mobility. For data interpretation, a band structure model offered in [11] was used.

This study continues the magnetotransport investigations that have been started by us on α''' -(Cd_{0.5}Zn_{0.5})₃As₂ at higher pressures. In [12], resistivity ρ , magnetoresistance $\Delta\rho_{xx}/\rho_0$ and Hall coefficient R_H were measured in (Cd_{0.69}Zn_{0.31})₃As₂ sample. At atmospheric pressure, the temperature dependence of the resistivity of (Cd_{0.69}Zn_{0.31})₃As₂ sample in the temperature range of 77–400 K is typical for the metallic type of conductivity: the

Hall coefficient is almost constant within the temperature range and negative sign of R_H is preserved which indicates that electrons are the main charge carriers. Such behavior is a typical characteristic of a semimetallic semiconductor. Another feature of the transport under pressure is in an increase in resistivity ρ [12]. The type of conductivity of (Cd_{1–x})₃Zn_xAs₂ matrix material depends strongly on the relation between Cd and Zn. Thus, in case when $x \geq 0.15$,

The p -type should be expected, rather than n -type, for (Cd_{1–x})₃Zn_xAs₂ matrix. α''' -(Cd_{0.5}Zn_{0.5})₃As₂ compounds represent a special case of cadmium arsenide compound Cd₃As₂ where zero-gap electron states near symmetry-protected Dirac points have linear dispersion and rigidly-bound spin and pulse directions [13]. However, the electron density in Cd₃As₂ may be decreased by doping with Zn atoms and (Cd_{1–x}Zn_x)₃As₂ crystals where $0 \leq x \leq 1$, form a continuous set of solid solutions. Due to variation of Zn concentration in (Cd_{1–x}Zn_x)₃As₂ system, transition from three-dimensional Dirac semimetal to trivial direct-band-gap semiconductor occurs at $x_c = 0.38$, and, within $0.07 \leq x < 0.52$, structural transformation of a tetragonal body-centered phase ($I4_1/acd$) to a primitive tetragonal phase ($P4_2/nmc$) takes place; then, at $x > 0.52$, the tetragonal body-centered phase is restored [14,15].

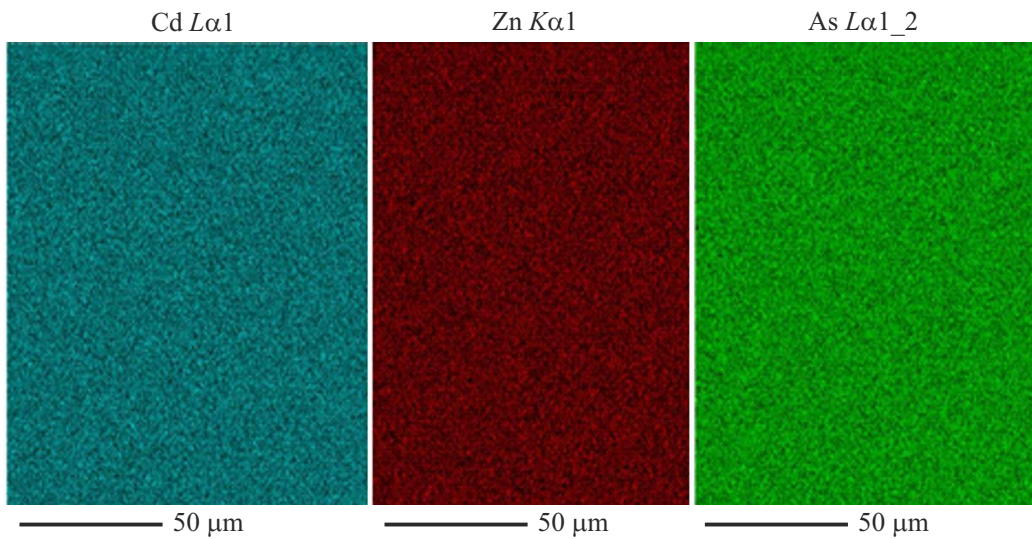


Figure 1. Uniform element distribution on α''' -($\text{Cd}_{0.5}\text{Zn}_{0.5}$) $_3\text{As}_2$ sample surface according to the energy-dispersive X-ray spectroscopy.

2. Experimental procedure

For pressurization, „Toroid“ [16] type chamber was used to apply hydrostatic pressure up to 9 GPa. Parameters of the α''' -($\text{Cd}_{0.5}\text{Zn}_{0.5}$) $_3\text{As}_2$ test sample: $\rho = 12 \Omega \cdot \text{cm}$, $n = 3.8 \cdot 10^{15} \text{ cm}^{-3}$.

Electron microscope investigations of chips and sample surfaces were performed using JSM6610LV (Jeol) scanning electron microscope with X-Max^N (Oxford Instruments) energy-dispersive X-ray spectroscopy (EDXRS) add-on module. The EDXRS data for α''' -($\text{Cd}_{0.5}\text{Zn}_{0.5}$) $_3\text{As}_2$ has shown that elements are evenly distributed in the sample (Figure 1).

X-ray diffraction analysis conducted using GBC EMMA (radiation $\text{CuK}\alpha$, $\lambda = 1.5401 \text{ \AA}$) X-ray diffractometer at room temperature has also confirmed the single-phase composition of the sample. The crystalline structure corresponds to α''' -polymorphous modification that was observed in [14,15] for some cadmium-zinc arsenide solid solutions. This structure is tetragonal (space group $I4_1/amd$) with $a = b = 8.55 \text{ \AA}$ and $c = 24.13 \text{ \AA}$.

3. Findings and discussion

In [12], resistivity ($\text{Cd}_{0.69}\text{Zn}_{0.31}$) $_3\text{As}_2$ demonstrates the dependence on temperature typical for metals.

Investigations of the transverse magnetoresistance $\Delta\rho_{xx}(P)/\rho_0$ ($\text{Cd}_{0.69}\text{Zn}_{0.31}$) $_3\text{As}_2$ in the pressure range up to 9 GPa with fixed magnetic field allowed to detect pressure intervals where negative magnetoresistance (NMR) is manifested. In the phase transition region, NMR at $P \approx 2.7 \text{ GPa}$ in 5 kOe field has a minimum approximate value of -0.17 .

In addition to NMR, features of positive magnetoresistance behavior also appear in the material of interest, with maximum magnetoresistance observed near 4 GPa.

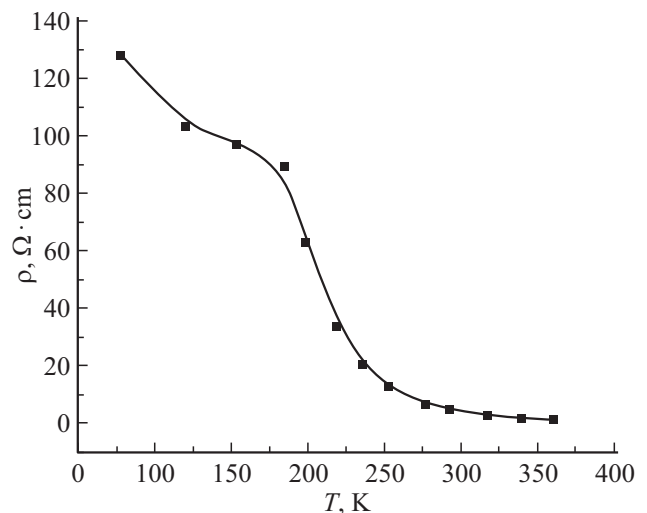


Figure 2. Temperature dependence of the resistivity $\rho(T)$ of α''' -($\text{Cd}_{0.5}\text{Zn}_{0.5}$) $_3\text{As}_2$ sample.

Further investigations of magnetotransport properties α''' -($\text{Cd}_{0.5}\text{Zn}_{0.5}$) $_3\text{As}_2$ were conducted in the range of 77–400 K and 0–9 GPa. Curve of the resistivity of α''' -($\text{Cd}_{0.5}\text{Zn}_{0.5}$) $_3\text{As}_2$ sample vs. temperature $\rho(T)$ is shown in Figure 2. This curve demonstrates the semiconductor behavior variation: the resistivity grows with temperature decrease. This temperature dependence differs drastically from that observed in [12] for ($\text{Cd}_{1-x}\text{Zn}_x$) $_3\text{As}_2$ ($x = 0.31$) sample.

The temperature dependence of the Hall coefficient R_H shows sign reversal. Therefore, holes are the main charge carriers from 77 K and to 200 K, and the semiconductor has p -type conductivity. Then, sign reversal of the main charge carriers takes place, electrons are the main charge carriers while the semiconductor demonstrates n -type conductivity.

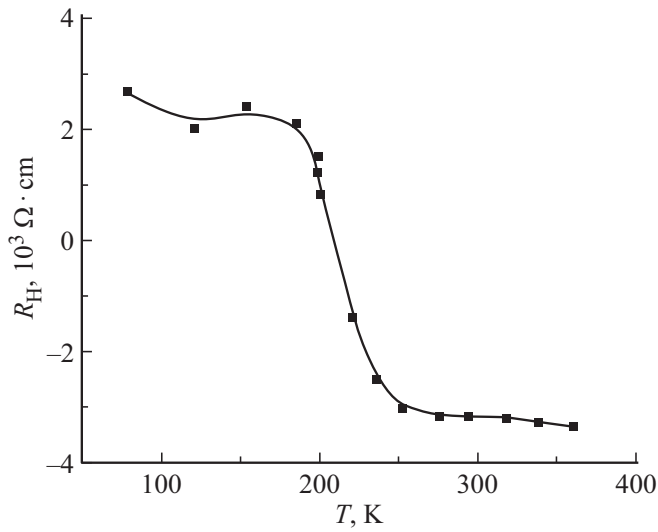


Figure 3. Temperature dependence of the Hall coefficient $R_H(T)$ $\alpha'''-(\text{Cd}_{0.5}\text{Zn}_{0.5})_3\text{As}_2$.

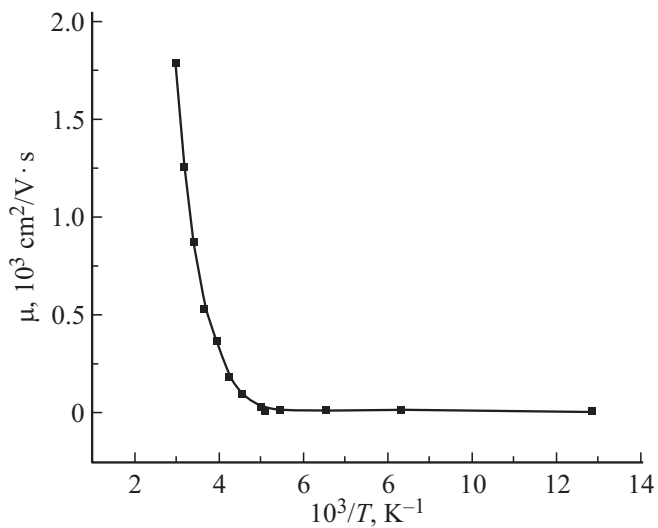


Figure 4. Temperature dependence of $(\text{Cd}_{0.5}\text{Zn}_{0.5})_3\text{As}_2$ mobility.

Resistivity drop with temperature rise in the sample is followed by the charge carrier mobility growth (Figure 4). Mobility growth in this case means an increase in the contribution to conductivity made by another group of charge carriers with a lower effective mass. In the range of $T < 200$ K, the Hall charge carrier mobility μ_H does not depend on temperature (Figure 4), and μ_H grows dramatically at $T > 200$ K.

The Hall coefficient that is weakly dependent on the temperature indicates that holes are that main current carriers at $T < 200$ K.

Baric dependencies of the resistivity $\rho(P)$, Hall coefficient $R_H(P)$ and magnetoresistance $\Delta\rho_{xx}(P)/\rho_0(P)$ $\alpha'''-(\text{Cd}_{0.5}\text{Zn}_{0.5})_3\text{As}_2$ at fixed magnetic inductions up to 5 kOe and room temperature are shown in Figure 5–7,

respectively. Transverse magnetoresistance was calculated using the following equation

$$\frac{\Delta R}{R_0} = \frac{R(B) - R(0)}{R(0)}, \quad (1)$$

where $R(B)$ and $R(0)$ are resistance in the transverse magnetic field with induction B and without any magnetic field, respectively.

Analysis of the data recorded in the pressure rise and relief conditions provided a reliable correlation between the MR behavior and observed hysteresis on $\rho(P)$. With the pressure growth, the resistivity $\alpha'''-(\text{Cd}_{0.5}\text{Zn}_{0.5})_3\text{As}_2$ grows non-monotonously, and in the range of $P \approx (2.8-3.5)$ GPa, maximum resistivity $\rho(P)$ is observed (Figure 5).

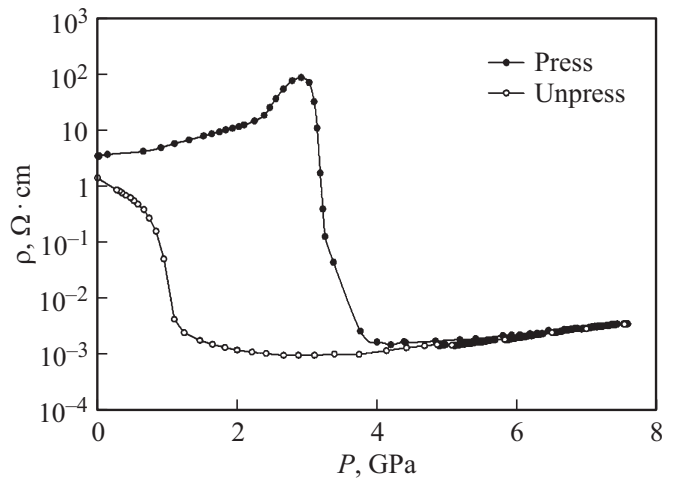


Figure 5. Baric dependence of the resistivity $\rho(P)$ of $\alpha'''-(\text{Cd}_{0.5}\text{Zn}_{0.5})_3\text{As}_2$.

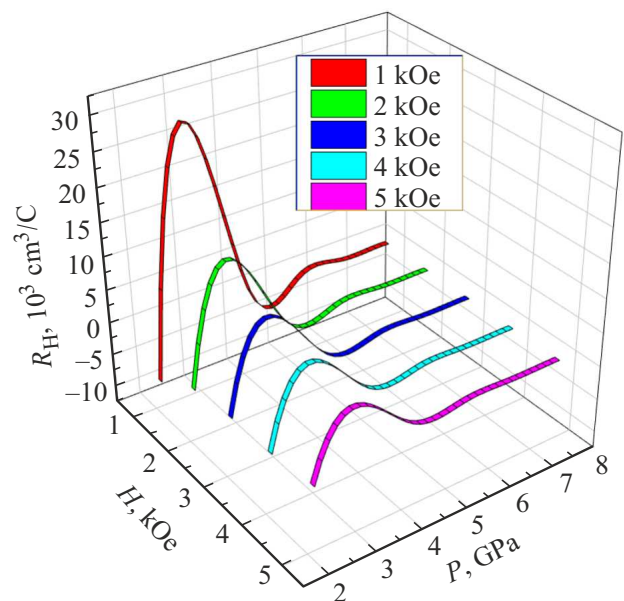


Figure 6. Baric dependences of the Hall coefficient $R_H(P)$ $(\text{Cd}_{0.5}\text{Zn}_{0.5})_3\text{As}_2$.

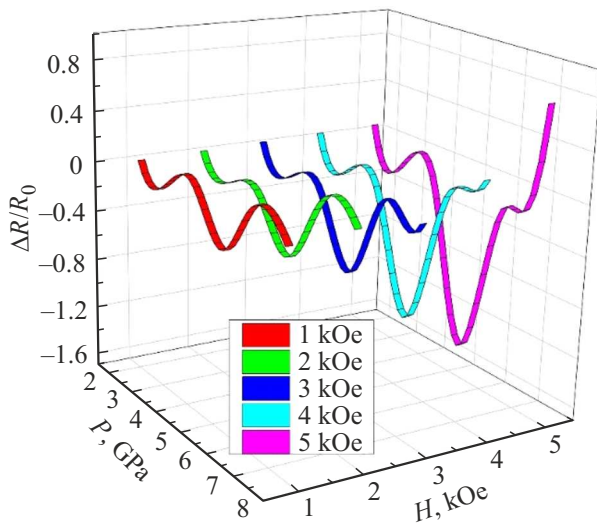


Figure 7. Dependences of the magnetoresistance of $(\text{Cd}_{0.5}\text{Zn}_{0.5})_3\text{As}_2$ composite on pressure at various transverse magnetic field strengths with pressure rise.

Hall coefficient $R_H(P)$ (Figure 6) achieves its peak in the pressure range of (2.5–3.5) GPa. With an increase in the magnetic field, the $R_H(P)$ peak amplitude decreases (Figure 6). After the pressure relief, the sample is not restored. The peak on $\rho(P)$ is probably attributed to the phase transition, but may be associated with the involvement of the second subband electrons in the conductivity, which is detected when the effect of the comprehensive pressure on the electrical properties of $\text{Cd}_{3-x}\text{Zn}_x\text{As}_2$ is investigated.

The temperature dependence of the Hall coefficient $R_H(T)$ shows the Hall coefficient sign reversal (Figure 3) from „+“ at low temperatures to „–“ with the temperature rise. With the pressure rise, the sign inversion point R_H moves towards weak magnetic fields. In the maximum pressure range, there is almost no any dependence of the Hall coefficient on the magnetic field.

Experimental dependences of the transverse magnetoresistance of $(\text{Cd}_{0.5}\text{Zn}_{0.5})_3\text{As}_2$ $\Delta\rho_{xx}(P)/\rho_0$ with fixed magnetic field strengths are shown in Figure 7. The magnetoresistances are negative at $P \geq 1.5$ and increase in the absolute value with the increase in the magnetic field. In $H = 1–5$ kOe fields at 4.0–4.7 GPa, a magnetoresistance jump is observed, their absolute values achieve their peak and then are decreasing. In 5 kOe field at 4.0–4.7 GPa, the negative magnetoresistance has its lowest value -1.5 (Figure 7).

Variation of the field dependence of the magnetoresistance is asymmetric about the field direction. Cd_3As_2 is known as one of the materials where the magnetoresistance parity may be violated under particular conditions. This may result both in slight asymmetry and in magnetoresistance chirality [13–17].

4. Conclusion

Temperature and baric dependences of α''' - $(\text{Cd}_{0.5}\text{Zn}_{0.5})_3\text{As}_2$ have been investigated. The temperature-dependent resistivity has been found to demonstrate the semiconductor behavior variation. The temperature dependence of the resistivity has a shape typical for semiconductors. On the temperature dependence of the Hall coefficient $R_H(T)$ within the range of 320–350 K, change of the types of carriers occurs — transition from *p*-type material to *n*-type material. It has been shown that the increase in pressure results in suppression of the positive magnetoresistance. In 5 kOe field at 4.0–4.7 GPa, the negative magnetoresistance has its maximum absolute value. Variation of the field dependence of the magnetoresistance is asymmetric about the field direction.

Complex resistivity and Hall coefficient behavior during temperature, pressure and magnetic field variation may be attributed to the band structure features, change of the Fermi level position against the energy band edges and impurity levels, and to the variation of the charge carrier concentration.

The electric field and temperature affects the number of free charge carriers, and the magnetic field and pressure change the energy bandgaps resulting, in turn, in the change of the number of carriers. As opposed to the electric field that directly changes the number of free charge carriers, the magnetic field causes rearrangement of the energy spectrum, i.e. results in displacement of the energy band edges.

Conflict of interest

The authors declare that they have no conflict of interest.

References

- [1] L. Zdanowicz, W. Zdanowicz. *Phys. Status Solidi* **6**, 227 (1964).
- [2] W. Zdanowicz, B. Trumpowski. *Acta Phys. Pol.* **24**, 1, 205 (1964).
- [3] A.K. Sreedhar. *J. Inst. Telecommun. Eng.* **9**, 268 (1963).
- [4] Ya.A. Ugai, T.A. Zyubina, E.A. Malygin. *Izv. AN SSSR. Neorgan. materialy* **17**, 876 (1966). (in Russian).
- [5] N.N. Sirota, E.M. Stolyarenko. *Izv. AN BSSR. Ser. fiz.-mat. nauk* **1**, 107 (1966) (in Russian).
- [6] J. Cisowski, W. Zdanowicz. *Phys. Status Solidi A* **19**, 2, 741 (1973).
- [7] J. Cisowski, W. Zdanowicz. *Phys. Status Solidi A* **41**, K59 (1977).
- [8] A.V. Lashkul, Yan Tsisovsky, E.K. Arushunova, A.F. Knyazev. *FTP* **23**, 8, 1406 (1989). (in Russian).
- [9] P.J. Lin-Chung. *Phys. Rev.* **188**, 1272 (1969).
- [10] M.J. Aubin, A.T. Truong. *Phys. Status Solidi A* **1**, 8, 217 (1972).
- [11] L.M. Rogers, R.M. Jenkins, A.J. Crocker. *J. Phys. D* **4**, 793 (1971).

- [12] L.A. Saipulaeva, V.S. Zakhvalinsky, A.G. Alikbekov. Poverkhnost', **10**, 76 (2023) (in Russian).
- [13] O. Ivanov, V. Zakhvalinskii, T. Nikulicheva, M. Yaprincev, S. Ivanichikhin. Phys. Status Solidi Rapid Res. Lett. **12**, 10, 1800386 (2018).
- [14] D.T. Son, B.Z. Spivak. Phys. Rev. B **88**, 125110 (2013).
- [15] S.A. Parameswaran, T. Grover, D.A. Abanin, D.A. Pesin, A. Vishwanath. Phys. Rev. X **4**, 031035 (2014).
- [16] Y.-Y. Zhang, X.-R. Wang, X.C. Xie. J. Phys. Condens. Matter **24**, 015004 (2012).
- [17] D.E. Kharzeev, H.-U. Yee. Phys. Rev. B **88**, 115119 (2013).

Translated by 123